RECLAMATION

Managing Water in the West

Hydraulic Laboratory Report HL-2009-07

Cavitation Potential of the Folsom Auxiliary Stepped Spillway

Laboratory Studies

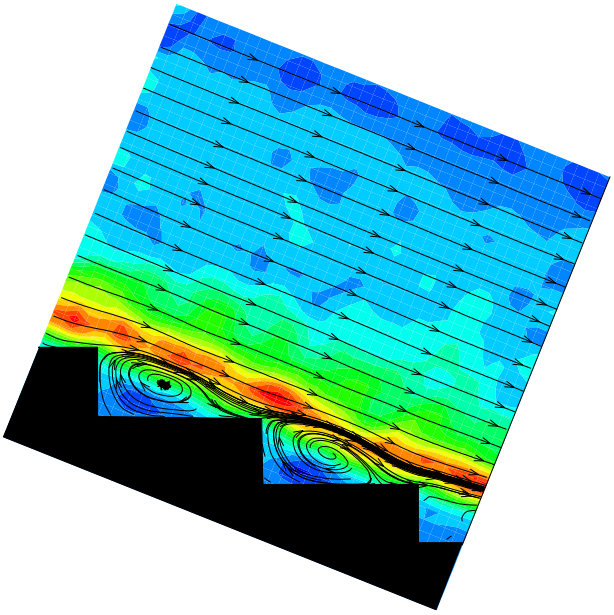

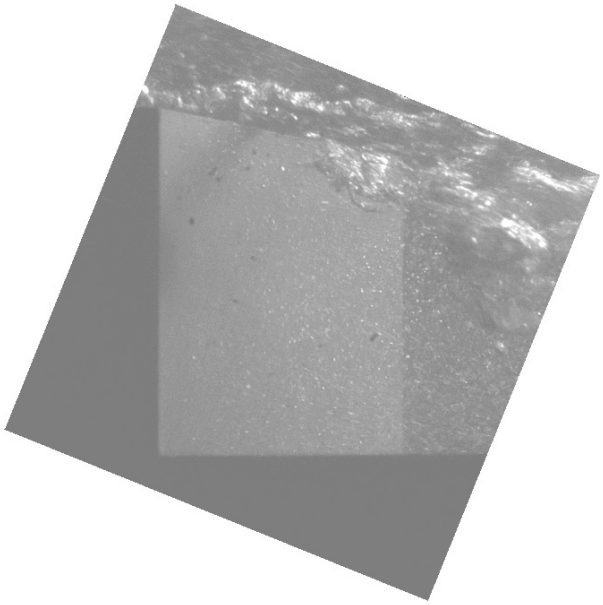

American River Division
Central Valley Project
Mid Pacific Region

U.S. Department of the Interior
Bureau of Reclamation
Technical Service Center
Hydraulic Investigations and Laboratory Group
Denver, Colorado

December 2009

REPORT DOCUMENTATION PAGE

Form Approved
OMB No. 0704-0188

1. REPORT DATE *(DD-MM-YYYY)*	2. REPORT TYPE	3. DATES COVERED *(From - To)*
December 2009	**Technical**	

4. TITLE AND SUBTITLE

Cavitation Potential of the Folsom Auxiliary Stepped Spillway

5a. CONTRACT NUMBER

5b. GRANT NUMBER

5c. PROGRAM ELEMENT NUMBER

6. AUTHOR(S)

K. W. Frizell and F. M. Renna

5d. PROJECT NUMBER

5e. TASK NUMBER

5f. WORK UNIT NUMBER

7. PERFORMING ORGANIZATION NAME(S) AND ADDRESS(ES)
U.S. Department of the Interior
Bureau of Reclamation, Technical Service Center
Hydraulic Investigations and Laboratory Services Group
DFC, 86-86460, PO Box 25007, Denver, CO 80225-0007

8. PERFORMING ORGANIZATION REPORT NUMBER

HL-2009-07

9. SPONSORING/MONITORING AGENCY NAME(S) AND ADDRESS(ES)
U.S. Army Corp of Engineers
Sacramento District – American River Design Section
CESPK-ED-DR
1325 J Street
Sacramento, CA 95814

10. SPONSOR/MONITOR'S ACRONYM(S)
USACE

11. SPONSOR/MONITOR'S REPORT NUMBER(S)

12. DISTRIBUTION/AVAILABILITY STATEMENT
National Technical Information Service (NTIS), 5285 Port Royal Road, Springfield, VA 22161. http://www.ntis.gov

13. SUPPLEMENTARY NOTES

14. ABSTRACT

Model studies were completed at Reclamation's hydraulic laboratory in Denver, CO to evaluate the cavitation potential of the stepped portion of the auxiliary spillway designed for the Folsom Dam JFP. The stepped spillway has a few unique features, including the uniform, high velocity flow that enters the stepped section. The constant-sloped reach (s = 0.4) was studied in a sectional model using 2 different step heights to simulate the relative roughness near the design and maximum PMF discharge conditions. Tests under atmospheric conditions investigated loss characteristics as well as detailed pressure and velocity fields with the use of Particle Image Velocimetry (PIV). The model was then moved to the laboratory's LAPC where reduced ambient pressures allowed measurement of the inception point for cavitation with visualization using high speed video. Test results compared well with the Darcy friction factor and the incipient cavitation index was determined for unaerated flow on a constant-sloped stepped spillway of 1V:2.5H.

15. SUBJECT TERMS
Folsom Dam, Joint Federal Project, stepped spillways, energy dissipation, friction factor, cavitation inception

16. SECURITY CLASSIFICATION OF:			17. LIMITATION OF ABSTRACT	18. NUMBER OF PAGES	19a. NAME OF RESPONSIBLE PERSON
					Robert Einhellig, Group Manager Hydraulic Investigations and Laboratory Services Group
a. REPORT	b. ABSTRACT	a. THIS PAGE			19b. TELEPHONE NUMBER *(Include area code)*
UL	UL	UL	SAR	32	303.445-2151

Hydraulic Laboratory Report HL-2009-07

Cavitation Potential of the Folsom Auxiliary Stepped Spillway

Laboratory Studies

American River Division
Central Valley Project
Mid Pacific Region

Prepared: K.W. Frizell
Research Hydraulic Engineer, Group 86-68460

Prepared: F.M. Renna
Visiting Scholar, Technical University of Bari, Italy

Technical Approval: Robert F. Einhellig, P.E.
Group Manager, Group 86-68460

Peer Review: Joseph Kubitscheck, P.E.
Hydraulic Engineer, Group 86-68460

12/29/2009
Date

U.S. Department of the Interior
Bureau of Reclamation
Technical Service Center
Hydraulic Investigations and Laboratory Group
Denver, Colorado

December 2009

Mission Statements

The mission of the Department of the Interior is to protect and provide access to our Nation's natural and cultural heritage and honor our trust responsibilities to Indian Tribes and our commitments to island communities.

The mission of the Bureau of Reclamation is to manage, develop, and protect water and related resources in an environmentally and economically sound manner in the interest of the American public.

Acknowledgments

Dane Cheek, Research Machinist constructed the lab model. Marty Poos and Jimmy Hastings provided construction support for the various modifications between the lab floor and LAPC. Sheena Barnes assisted greatly in the data collection and organization.

Hydraulic Laboratory Reports

The Hydraulic Laboratory Report series is produced by the Bureau of Reclamation's Hydraulic Investigations and Lab Services Group (Mail Code 86-68460), PO Box 25007, Denver, Colorado 80225-0007. At the time of publication, this report was also made available online at **http://www.usbr.gov/pmts/hydraulics_lab/pubs/HL/HL-2009-07.pdf**

Disclaimer

No warranty is expressed or implied regarding the usefulness or completeness of the information contained in this report. References to commercial products do not imply endorsement by the Bureau of Reclamation and may not be used for advertising or promotional purposes.

Cover Photo: Left image is PIV data of streamlines and Turbulent Kinetic Energy production at the scaled velocity of 6 m/s, right image is at similar velocity and shows cavitation bubbles and vortices within the shear layer just above the step tips.

Funding was provided by the USACE-Sacramento District

Contents

Figures

Tables

Glossary of Symbols and Terms

AE – acoustic emissions
COE – US Army Corps of Engineers
FFT – fast Fourier transform
JFP – Joint Federal Project
LAPC – low ambient pressure chamber
PIV – particle image velocimetry
RCC – roller-compacted concrete
RMS – root mean square value
TKE – turbulent kinetic energy
Reynolds Number – inertial forces/viscous forces - $\frac{VD_h}{\nu}$
Euler Number – dimensionless pressure coefficient - $\frac{\Delta p}{\frac{1}{2}\rho V^2}$
Weber Number – inertial forces/surface tension forces - $\frac{\rho V^2 L}{\sigma}$
A – cross-sectional flow area
D_h – hydraulic diameter – $4R_h$
H – height of test section
P – pressure
P_o – reference pressure
P_v – vapor pressure of water
Q – discharge
R_h – hydraulic radius – cross sectional area/wetted perimeter
S_{xy} – shear rate of strain
U – mean streamwise velocity
V – mean vertical velocity
V_o – reference velocity
W – width of test section
f – Darcy friction factor
f_b – bottom friction factor
l – length of step tread (horizontal)
h – height of step tread (vertical)
s – slope
q – specific (or unit) discharge
u – fluctuating streamwise velocity
u' – RMS of the streamwise fluctuations
v – fluctuating vertical velocity
v' – RMS of the vertical fluctuations
$-\overline{uv}$ –component of Reynolds stress
γ_g – geometric scale factor
ε – rugosity or roughness height perpendicular to slope ($h\cos\theta$)
$\frac{e}{D_h}$ - relative roughness
ζ_z – mean spanwise vorticity
θ – angle of slope from horizontal
ρ – density of water
σ – cavitation parameter
σ_i – inception cavitation parameter

Summary

Tests were conducted at Reclamation's Denver laboratory to investigate the cavitation potential of a novel stepped spillway designed for the Joint Federal Project (JFP) at Folsom Dam, California. The auxiliary spillway design includes a control structure which is comprised of six top-seal radial gates with a crest elevation of 112.17 m (368.0 ft) at the reservoir to regulate releases through the downstream spillway chute. The auxiliary spillway chute is a concrete channel that is 51.5-m-wide (169 ft) with a constant slope s = 0.02 for a distance of approximately 610 m (2,000 ft) downstream of the control structure. At that point the chute becomes stepped with a slope that parabolically increases to s = 0.4025 over a distance of approximately 122 m (400 ft) downstream of the first step. Along this reach of increasing slope, the step heights also increase to the maximum offset of 0.98-m (3-ft) which is maintained downstream until the chute terminates in the stilling basin at elevation of 39.03 m (128.05 ft). The constant sloped section at s = 0.4025 is about 83.8-m-long (275-ft). The design discharge of the auxiliary spillway is 3823 m^3/s (135,000 ft^3/s) with a maximum flow of 8835 m^3/s (312,000 ft^3/s).

The sectional model of the constant slope stepped reach of the auxiliary spillway featured a closed rectangular conduit (0.203-m by 0.203-m [8-in by 8-in]) with steps along the bottom. The flume was placed horizontally so that the lid of the flume would represent a surface parallel to the slope of the steps. Two sets of steps were tested, one with a roughness height ε = 50.8 mm (2-inches), giving a relative roughness ε/D_h of 0.256 and then one with ε = 25.4 mm (1-inch) for a relative roughness ε/D_h of 0.128 with double the number of steps as the previous arrangement. The larger steps are a good representation for the design discharge condition while the half-height steps represent the conditions of the maximum discharge. Flow entered the test section through a transition with smooth parabolic curves and straightening vanes attached to a pressure tank. Piezometer taps along the lid allowed measurement of the pressure gradient along the steps that was used to calculate the friction factor. In both test locations, the lab floor and the LAPC, flows up to 0.255 m^3/s (9 ft^3/s) were possible. On the laboratory floor, all pressure measurements were collected both on the lid and at three sets of steps. In addition the velocity profile entering the test section was measured with a Prandtl tube. Particle Image Velocimetry (PIV) was acquired at the three instrumented step locations for the range of flow rates tested. Within the LAPC, acoustic emissions were used to indicate cavitation presence and strength. High-speed video was also used to document the physical appearance and location of the cavitation within the model.

Estimates of friction factor from two basic methods compared well. A "global" approach featured using the energy loss over the entire test section to compute a Darcy friction factor and then applied weight factors to correct for the roughness being only on the bottom surface of the rectangular conduit. In addition, a "local" approach used the PIV measurements, extracting velocity profiles throughout the test section at various locations and then applying both power law and logarithmic law models to compute friction factor. These were also checked against several other commonly used methods that appear in the literature. The larger steps (larger relative roughness) had friction factors of 0.166 to 0.160 for the local and global approaches, respectively. The smaller steps had friction factors of 0.091 to 0.094 for the local and global methods, respectively. These values compared favorably to the design approach with mean values reported by the U.S. Army Corps of Engineers (COE), using a bottom friction factor developed by Boes and Hager (f_b=0.12 for the larger relative roughness and 0.095 for the smaller relative roughness).

Cavitation inception appeared first within the shear layer just above the step tips. The PIV measurements identified this region as the location of the highest vorticity and turbulent kinetic energy production. These incipient values can then be compared to the flow sigma calculations along the spillway profile for different discharges. It should be noted that all lab data were collected in unaerated flow conditions, somewhat atypical of stepped spillway prototype performance experience. The large specific discharges for the Folsom design and maximum flow cases could lead one to question if aeration takes place and if so, at what discharges it occurs. The previous scale physical models (1:26 and 1:48) tend to suggest that at flow rates up to and including the design flow that some aeration on the stepped portion of the chute could be present. However, it is unlikely that at the maximum discharge that any aeration will be present.

Introduction

The design of stepped spillways has been the topic of many research studies and publications over the past 30 years. The use of stepped spillways has become more prevalent largely due to the impacts that roller-compacted concrete (RCC), have had on dam construction and remediation techniques. The standard placement technique of RCC involves relatively small lifts of low-slump concrete, leaving a stepped profile, a natural lead in to the use of a stepped chute as a spillway. Steps for the spillway chute are generally formed by some method (traditional forming, slip forms, curbing machines, etc.) rather than leaving the rough unfinished steps characteristic of RCC construction, The use of steps on the spillway surface and their advantage in energy dissipation, especially for low dams with low to moderate specific discharges, has made them a cost-effective alternative to traditional formed reinforced smooth concrete spillways.

The energy dissipation benefit of a stepped versus a smooth chute has been documented many times over (Chanson [2001], Matos [2000], Outsu and Yasuda [1997]). Their use has become common on low head structures and they have performed well in many locations for many years. Their use in high-head spillways or large specific discharge spillways has still been somewhat limited. The combination of deep flows and high velocities has been the cause for concern over possible cavitation damage on stepped chutes. To date there has not been evidence that a stepped chute has experienced cavitation damage, however new designs are pushing the extremes of velocity and depths, yielding concerns about air entrainment and its role in protection of the stepped chute from cavitation damage. Most high-head structures that have been constructed to date have featured very steeply sloped stepped chutes (50- to 60-degrees), and the relatively small specific discharges have guarantee fully aerated flow conditions.

The Folsom auxiliary spillway has several features that make it a unique structure among stepped spillways. The control structure is a set of 6 top-seal tainter gates, with a maximum head of slightly over 30.5 m (100 ft). The gates discharge onto a smooth chute 637-m-long (2090-ft) with a slope of 0.02. The chute then begins a parabolic transition to a constant slope of 0.4025. As the parabolic transition begins, the steps begin and vary in height from roughly 0.23 m (0.75 ft) up to 0.98 m (3 ft). Unlike traditional stepped chutes which usually have an ungated ogee crest, a very high velocity is achieved in the smooth chute prior to the water encountering the steps. The other feature that is well beyond the typical design values used previously is the specific discharges at design and maximum flow, 74 m^2/s (800 ft^2/s) and 172 m^2/s (1,850 ft^2/s) respectively. The majority of structures that have been designed previously have had specific discharges less than about 28 m^2/s (300 ft^2/s); the typical case being below 10 m^2/s (100 ft^2/s). These low specific discharges result in very large relative roughnesses such that achieving a fully aerated flow condition, which reduces or eliminates cavitation damage potential, has never been an issue of concern.

Methods and Materials

A closed conduit test section featuring steps representative of the constant-slope reach for the Folsom auxiliary spillway geometry was constructed and tested at Reclamation's laboratory in Denver, CO. Initial tests involved installing the test section on the laboratory floor. The conduit was attached to a pressure tank and flow was transitioned

into the rectangular conduit. Flow passed through the test section and into a tailbox with an adjustable water level. Figure 1 shows the model, as-installed on the laboratory floor.

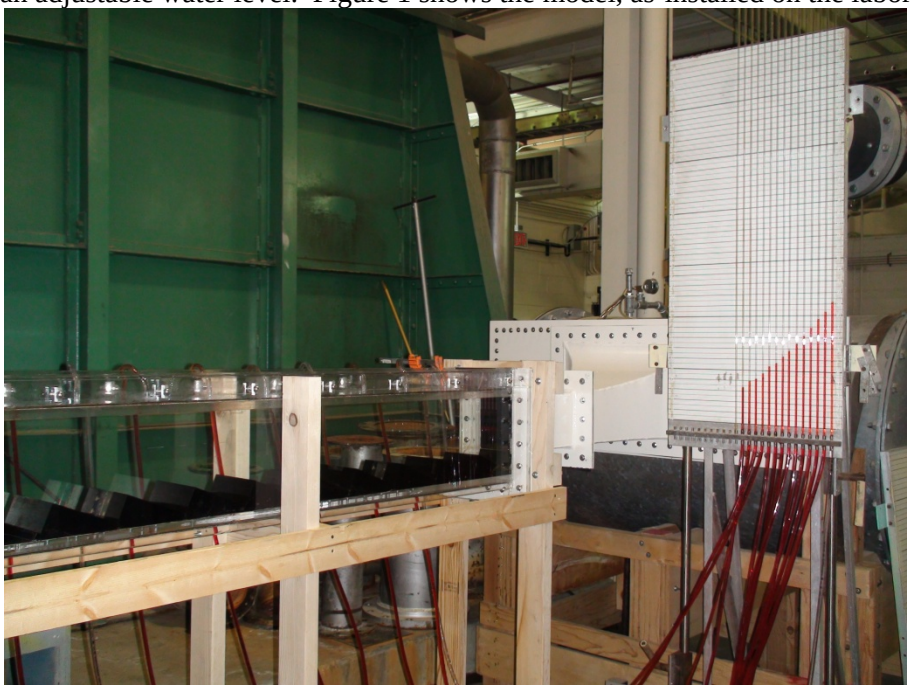

Figure 1: Test section containing Folsom steps installed on lab floor of Reclamation's laboratory. Large steps in place, ε = 50.8 mm (2 in).

The steps were oriented horizontally with the correct aspect to simulate Folsom's constant-sloped (0.40) lower portion of the auxiliary spillway, figure 2. Details of the step and test section dimensions are shown on Table 1. With this type of arrangement, the fixed lid could represent a water surface parallel to the slope. However as with any closed system, a pressure gradient unlike a free surface flow is present. Fourteen pressure taps equally spaced along the centerline of the lid allowed measurement of the pressure gradient (note manometer board on right side of figure 1) and hence computation of energy losses as well as reference pressures at points along the test section for determining the cavitation parameter. This pressure gradient information is used in a similar way that flow depths would be used in an open channel flow field. Three steps (steps 4, 9, and 14) along the conduit were instrumented with pressure taps along a step-riser and tread, figure 3. These step pressures were measured using manometer boards. Average hydrostatic pressures were attained through the reading and averaging of several digital photographs that instantaneously captured all the readings simultaneously. Flow rates were tested increasing from 0.057 m^3/s (2 ft^3/s) up to 0.255 m^3/s (9 ft^3/s) in increments of 0.028 m^3/s (1 ft^3/s).

Table 1: Test section conduit and step dimensions. See figure 2 for definitions.

	H mm(in)	W mm(in)	h mm(in)	l mm(in)	ε mm(in)	ϑ degrees
Large Steps	203.2 (8.0)	203.2 (8.0)	54.71 (2.15)	136.79 (5.39)	50.8 (2.0)	21.8
Small Steps	177.8 (7.0)	203.2 (8.0)	27.36 (1.08)	68.39 (2.69)	25.4 (1.0)	21.8

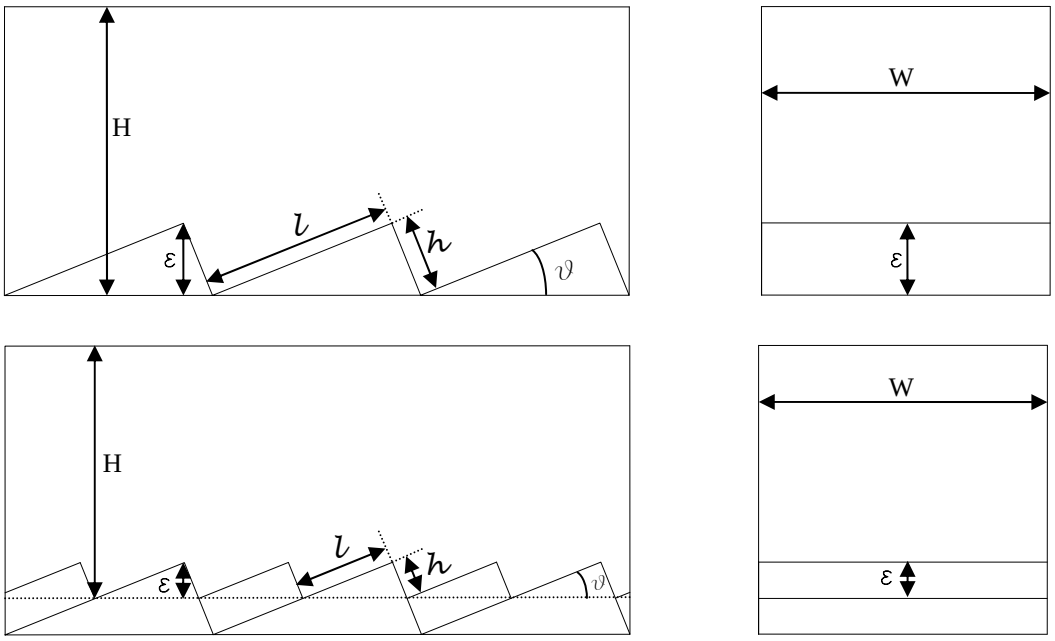

Figure 2: Details of model dimensions, large steps on top, smaller steps below. D_h, the hydraulic diameter is given by 4(WH/2W2H), this is 4 times the hydraulic radius.

Similitude considerations and practical limitations are typically used to define the model size. The present model was used to collect velocity and pressure data at atmospheric conditions and also to collect cavitation inception and formation data at reduced ambient pressure conditions in the laboratory's low ambient pressure chamber (LAPC). This does not imply that the closed-conduit sectional model simulates the open-channel stepped spillway in all manners. Ideally to represent an open channel stepped spillway, this would require equal Froude number and Euler number for the model and the prototype to be simultaneously satisfied. As we are working in a closed conduit the above is not possible; however we can choose a geometric ratio to attempt to best simulate a specific flow condition, i.e. the design discharge. Based on limitations in available discharge capacity and atmospheric pressure reduction within the LAPC, we attempted to choose the largest step dimensions in order to simulate the relative roughness (ε/D_h) at the design flow. The large steps, ε = 50.8 mm (2 in), result in a geometric scale of γ_g = 16.7. Using the geometric scale for the large steps, Euler number similitude between the model and the prototype can be realized if the ambient pressure in the chamber is reduced to 6.0-percent of the prototype value (the lowest capable by our installation). The small steps were fashioned as ½ the size of the large steps to facilitate easy installation and removal from the model. From a scaling perspective the relative roughness of the small steps represents close to the maximum discharge; however true Euler number similitude is not possible at the resulting scale factor (3-percent of the atmospheric pressure). The determination of the incipient cavitation index, σ_i, should largely be a function of the geometry under test. For instance, for a similar geometry, you are able to reproduce the incipient cavitation index with a variety of ambient pressures; this is the basis of using the LAPC. In the case of a typical atmospheric pressure versus 1/10th of that pressure, the resulting velocity needed at the reduced pressure in order to reach an equivalent σ_i value must be reduced by a factor of $\frac{1}{\sqrt{10}}$ of the velocity at atmospheric conditions.

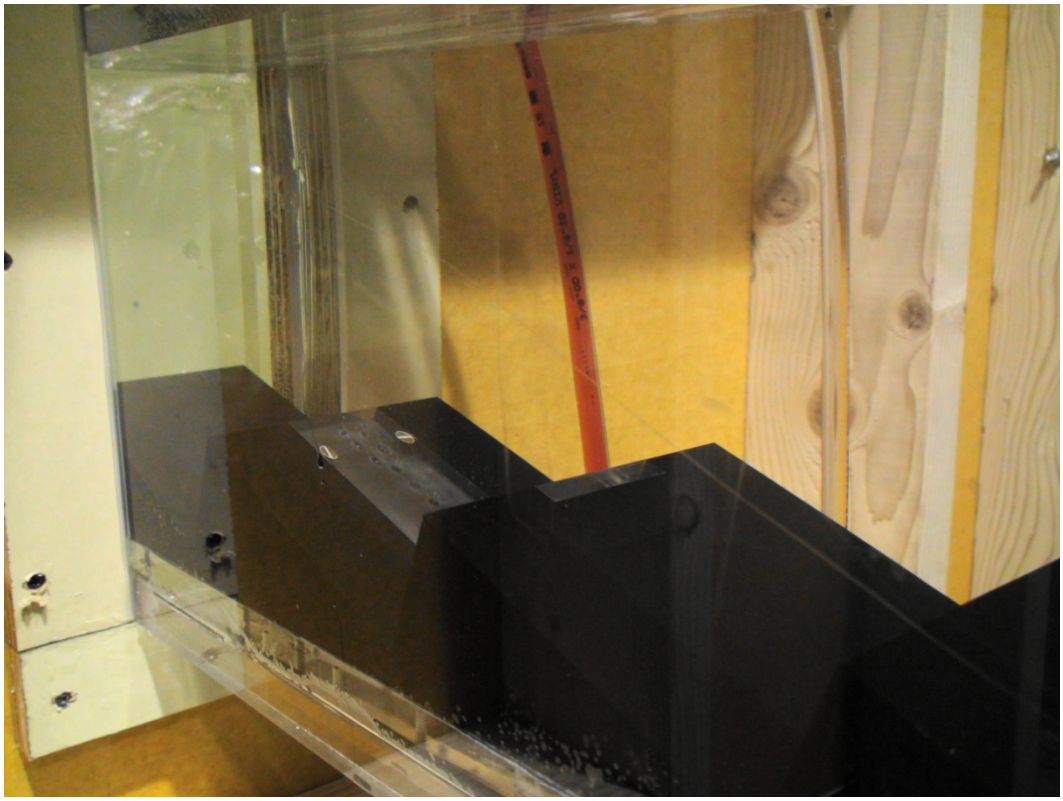

Figure 3: Step with piezometer taps. Total of 20 taps (1.5-mm-diameter (1/16-in-diameter)) were located along tread and adjacent riser.

The incoming vertical velocity profile along the centerline of the conduit was measured using a Prandtl tube (pitot-static), figure 4. These measurements were made to assess uniformity of the profile entering the test section. The differential pressure on the Prandtl tube (total head-static head = velocity head) was measured using a 34.5 kPad (5 psid) Sensotec model A-5/882-12A5D pressure transducer with an accuracy 0.25-percent full scale. A Sensotec Model GM signal conditioner was used, outputting a voltage-proportional pressure to an HP 3457A Multimeter, configured to output an average of 100 readings per measurement.

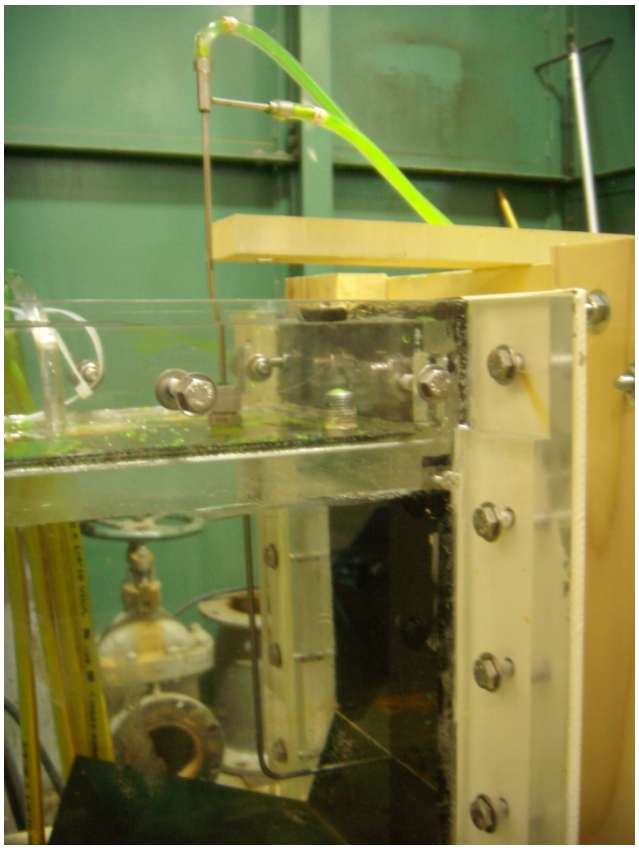

Figure 4: Prandtl tube used to measure vertical velocity profile on the conduit centerline. Pressure differential was measured with a Sensotec pressure transducer with an averaging voltmeter.

In addition, a 2-dimensional particle image velocimetry (PIV) system manufactured by DANTEC Dynamics was used to capture velocity fields near the conduit centerline at the 3 steps that were also instrumented with piezometer taps. The PIV system is a nonintrusive laser-based optical technique that captures whole-field instantaneous velocity vector measurements in a region of the flow. The system uses ensembles of digital photograph pairs taken with a camera that is synchronized with a pulsed laser sheet used to illuminate particles in the flow field. The pair of images is separated by a known time (typically 100-200 μs depending on velocity) such that correlation techniques can be used to track particles moving between successive frames and compute a resulting velocity vector. Numerous image pairs can be used within a single measurement to allow for an improved statistical definition of the flow present and computation of an extended set of flow-related properties. Typically 100 image pairs were used to define a measurement at each location with a maximum rate of 7.5 Hz. Prior to the collection of data, important parameters (interrogation area size and overlapping, FFT filter, and validation of signal peaks) were set in a group of trial runs spanning the range of velocities that would be expected. Figure 5 shows a view of the laser, mounted above the test section. This allows a planar sheet of illumination to be projected though the clear acrylic lid and then imaged through the clear side windows to obtain streamwise and vertical velocity components. The camera position was adjusted to allow imaging of the entire height of the test section and a width slightly more than one of the large steps or about 3 of the half-height steps.

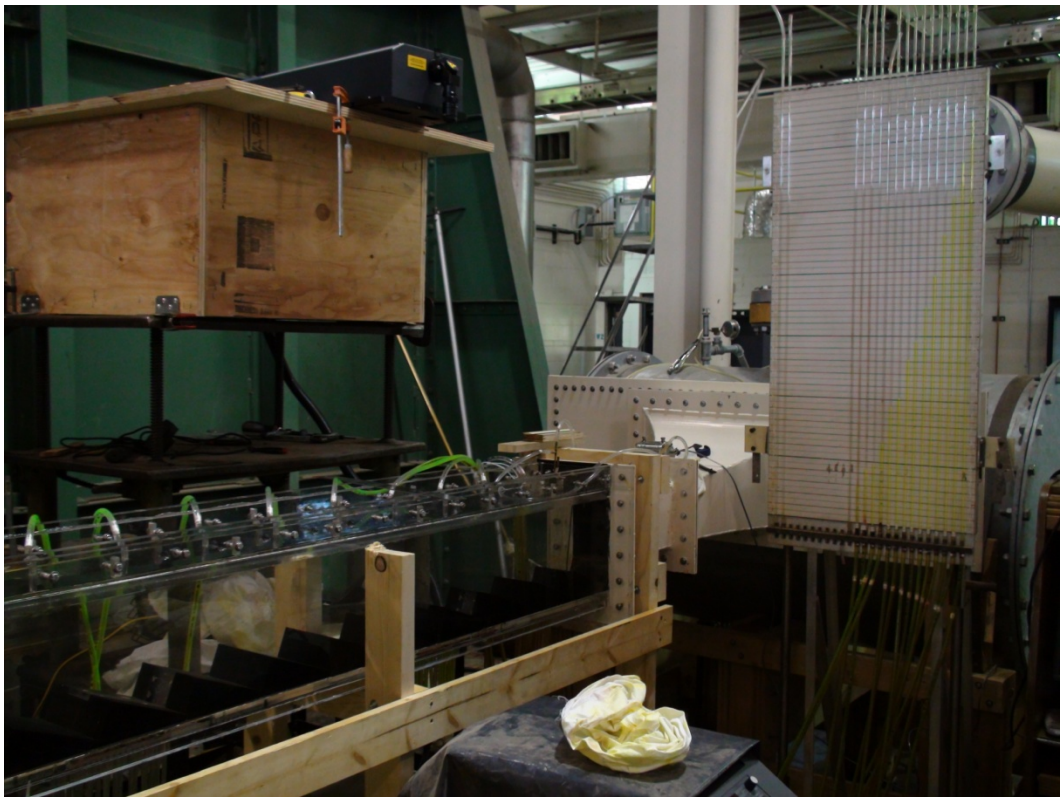

Figure 5: View of laser mounted above test section. Camera is mounted on the same cart but on the backside of the conduit. The entire setup was draped in black plastic during data collection to limit extraneous light noise and also for safety.

Following the initial testing on the lab floor to obtain pressure and velocity data, the acrylic conduit with steps and the pressure tank transition were moved to the LAPC. The LAPC is a permanent facility at the hydraulics laboratory that allows operating the model at a reduced ambient pressure for scaling of the cavitation parameter (a modified Euler Number). Figure 6 shows a view of the LAPC with the acrylic conduit in place. The LAPC is a recirculating closed system with an inline split-case pump. The downstream end of the conduit exited into a free-surface reservoir that was maintained behind a bulkhead wall within the chamber. Once the chamber was filled with city water, the vacuum pump was started and water circulated at a low rate for a period of 4-8 hours. This time period allowed the free gas to be removed from the water through the free surface; however the water remains close to saturation. At the end of this period, the pressure within the chamber was usually at its minimum sustainable value, about 71-73.5 kPa of vacuum. This value was somewhat dependent on how well the chamber re-sealed after each time it was returned to atmospheric conditions. The object of the LAPC tests was to determine the incipient cavitation index and also observe the formation, location, and intensity of cavitation within the model for various values of the cavitation index. Acoustic emission activity was recorded for an increasing velocity within the test section as the ambient pressure was maintained constant (lowering σ, the cavitation parameter). This facility uses permanently installed instrumentation to measure discharge (electromagnetic flowmeter) and ambient pressure within the chamber. The local atmospheric pressure is measured adjacent to the facility using a NovaLynx Model 230-7410 Fortin-type barometer (accuracy ±0.25 mm-Hg (0.01 in)). Vapor pressure was determined from a temperature-based fitted curve for pure water using the measured

water temperature at the time of the run. In addition, we used an acoustic emissions sensor to indicate cavitation activity. The AE sensor was a DECI Model SE9125-M, a mass-loaded transducer that is equally sensitive to both extensional and flexural waves. The sensor was located adjacent to the last complete step within the conduit. The influence of the pressure gradient will initially force cavitation at this location. The signal conditioner was a DECI AESMART Model 302A and provided sampling of the signal in two different bandwidths of frequency, a low-frequency BW (20 kHz- 70 kHz), and a high-frequency BW (100 kHz – 1 MHz). The extensional and shear waves always appear in the high frequency bandpass and the flexural waves in the lower frequency bandpass. A counting technique was used to quantify the activity in each of these frequency bands by noting the number of times a threshold level was exceeded. The cavitation parameter (Eq. 1) calculation used a reference velocity equal to the mean velocity within the test section calculated as $V_o = Q/A$, and the reference pressure from the pressure gradient measurements taken on the lab floor.

$$\sigma = \frac{P_o - P_v}{\rho V_o^2 / 2} \tag{1}$$

The pressures are referenced to absolute zero pressure. This pressure decreased along the test section, yielding lower values of the Euler number from upstream to downstream along the conduit. High-speed video was collected using a Vision Research Inc. Phantom v4.2 digital camera and associated software. A macro/zoom lens allowed close up imaging from outside the chamber through the acrylic windows. All video was collected at a rate of 2000 frame/s, and replayed at much slower rates in order to visualize the details of cavitation formation and progression. Still images were captured from the video.

Figure 6: Low ambient pressure chamber (LAPC) with stepped test section installed inside the sealed vacuum chamber.

Results

Test results will be divided into two sections; lab floor tests where the conduit was tested under atmospheric conditions measuring pressure and velocities, and LAPC, where the conduit was exposed to a reduced ambient pressure in order to force cavitation at the reduced flow velocities in the model. All results unless specified otherwise are reported in model dimensions.

Atmospheric Tests – Laboratory Floor

The velocity information was acquired using PIV at the three instrumented steps. A data set of 100 image pairs was used in the data presentations included in this report. Samples of the type of data that can be calculated using the PIV measurements are shown in figures 7 and 8, for the 50-mm-high, and 25-mm-high steps respectively. The flow conditions presented roughly represent the design discharge of 3823 m^3/s (135,000 ft^3/s) with the 50-mm-steps, and the maximum flow of 8835 m^3/s (312,000 ft^3/s), with the 25-mm-steps. The x-axis is parallel to a line connecting the step tips, with the y-axis perpendicular to that line, representing the streamwise and vertical reference frame.

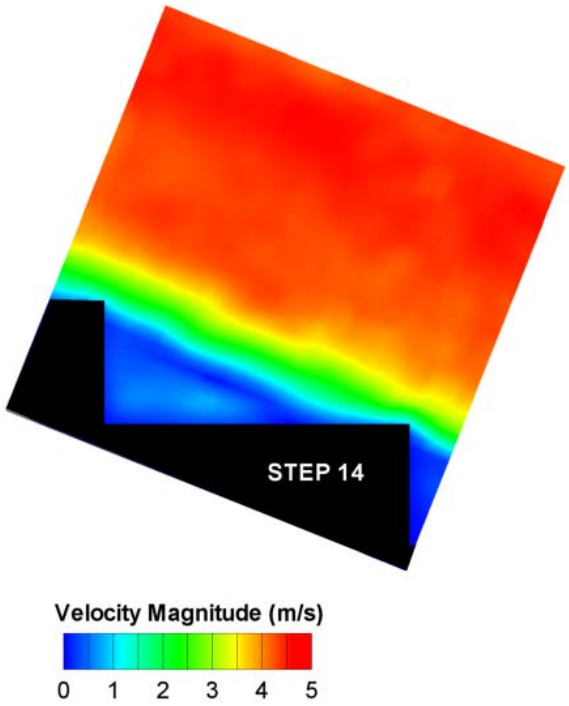

Figure 7a: Velocity vector magnitude from PIV measurements - model discharge is 0.1133 m^3/s (4 ft^3/s), maximum velocity ~5 m/s (16 ft/s).

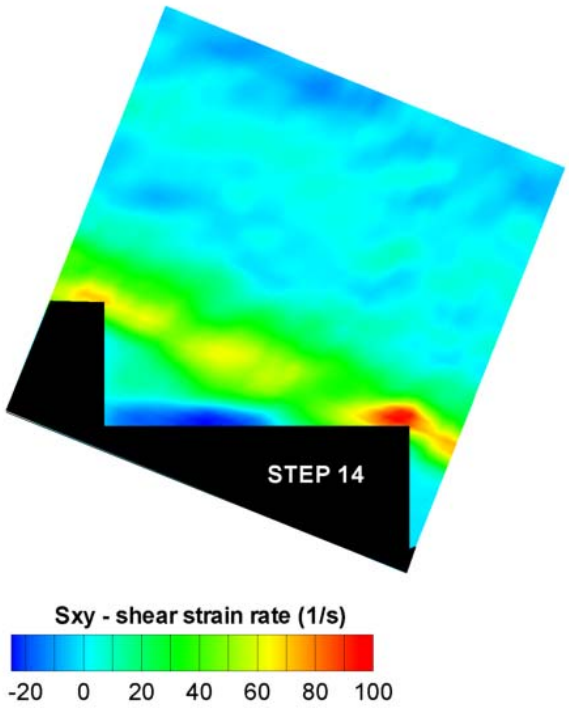

Figure 7b: S_{xy} - shear strain rate ([dU/dy+dV/dx]/2), symmetric part of the deformation tensor.

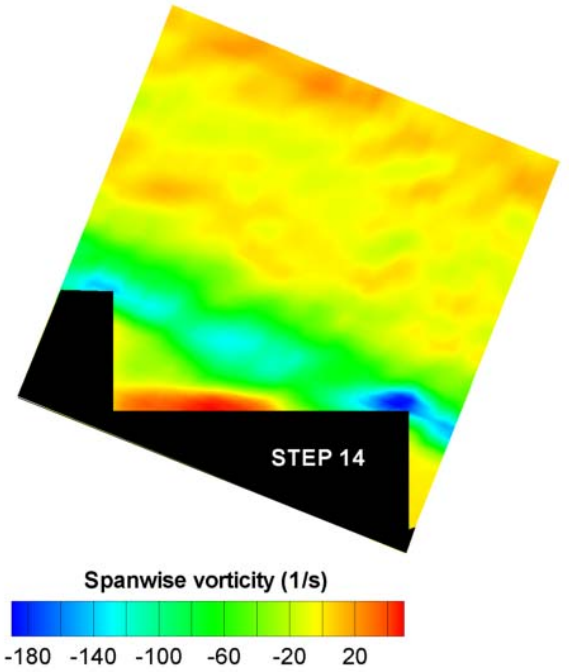

Figure 7c: Mean vorticity ζ_z (dV/dx-dU/dy), the skew symmetric part of the deformation tensor.

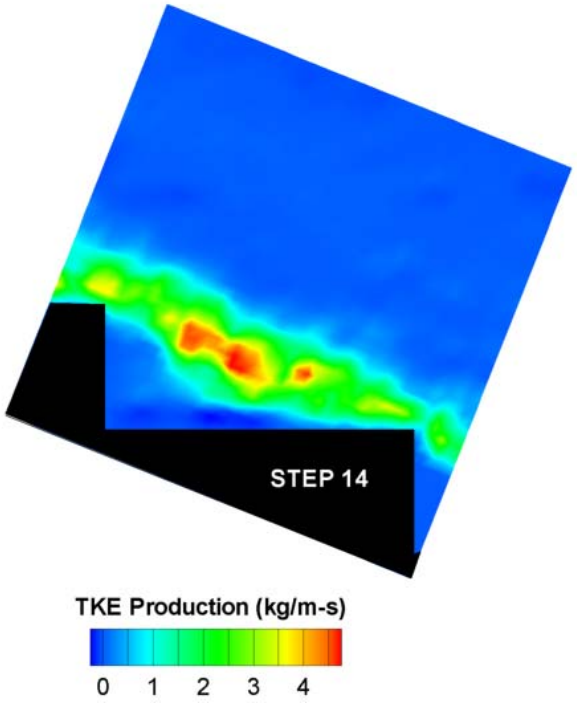

Figure 7d: Turbulent kinetic energy, calculated using the estimate of $-\overline{uv} \cong 0.4u'v'$ (where *u* and *v* are the fluctuating components and the prime denotes RMS of the variable).

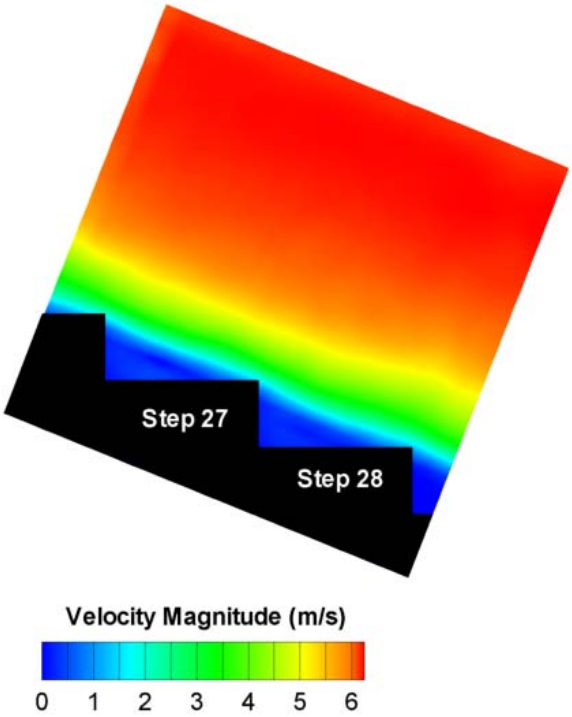

Figure 8a: Velocity magnitude from PIV measurements - model discharge is 0.1699 m^3/s (6 ft^3/s), maximum velocity ~6.4 m/s.

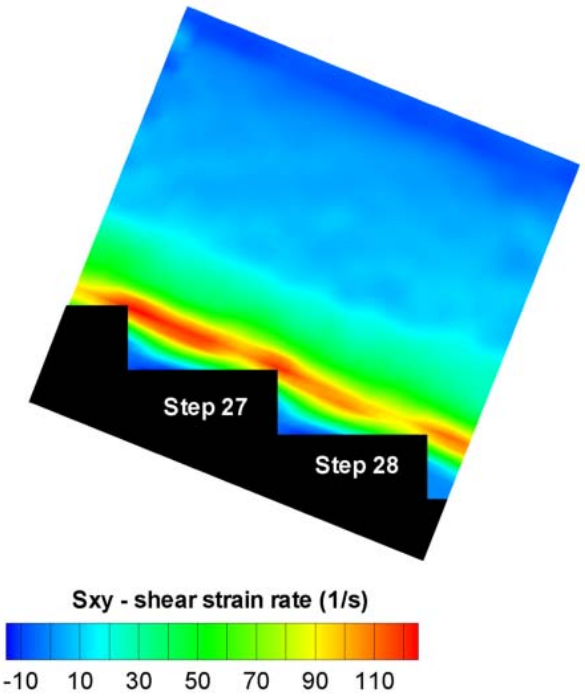

Figure 8b: S_{xy} - shear strain rate ([dU/dy+dV/dx]/2), symmetric part of the deformation tensor.

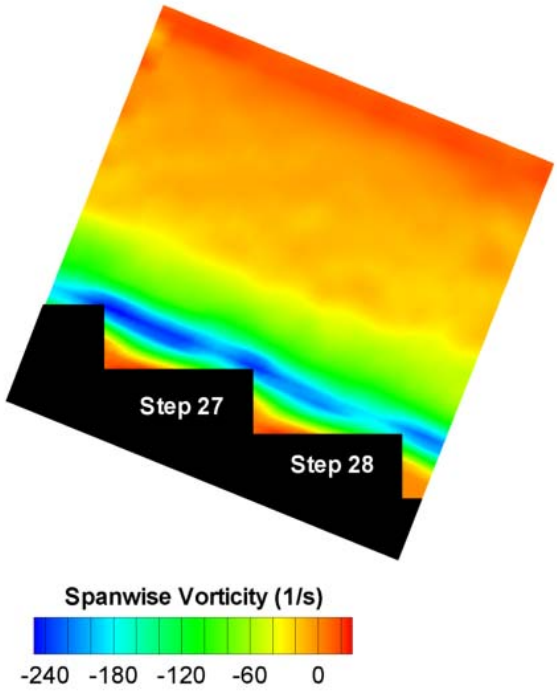

Figure 8c: Mean vorticity ζ_z (dV/dx-dU/dy), the skew symmetric part of the deformation tensor.

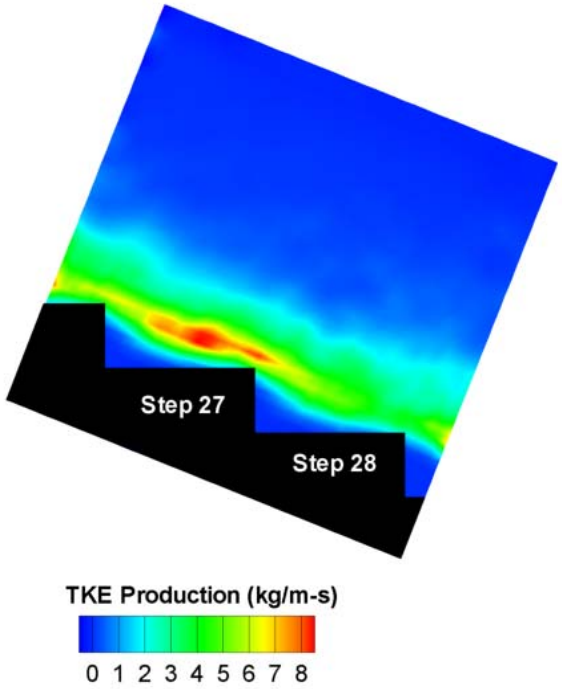

Figure 8d: Turbulent kinetic energy, calculated using the estimate of $-\overline{uv} \cong 0.4u'v'$ (where *u* and *v* are the fluctuating components and the prime denotes RMS of the variable).

The PIV data shown above can be used for specialized computations by extracting data from the data fields, such as velocity, figure 9. These data can then be used to determine friction along the steps using a power law or law of the wall logarithmic approach.

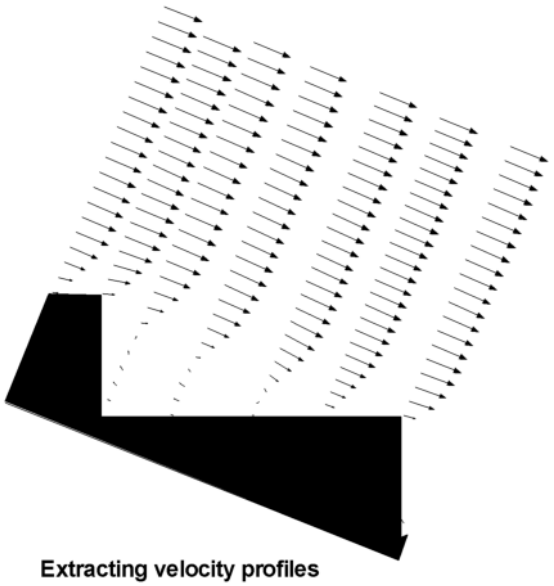

Figure 9: Velocity profiles extracted along lines within the interrogation area of the PIV data.

Pressure data were collected for all flow conditions tested. Figure 10 shows the pressure gradient on the lid for the 50 mm steps. Reference pressures were extracted from this data for each flow condition and step location.

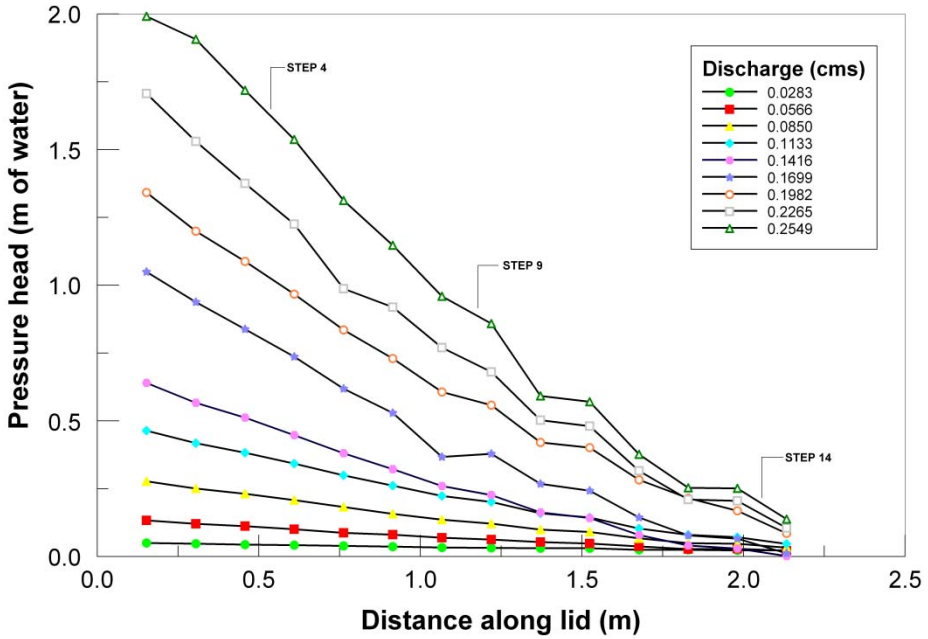

Figure 10: Pressure head on lid along stepped conduit (50-mm-high steps). Values of pressure at a specific discharge and step location are used as reference pressures.

Pressures on the steps were also collected and data for the design discharge are presented in figure 11. These data are in non-dimensionalized form, normalized using the appropriate reference pressure as described above. No negative pressures were observed at this condition.

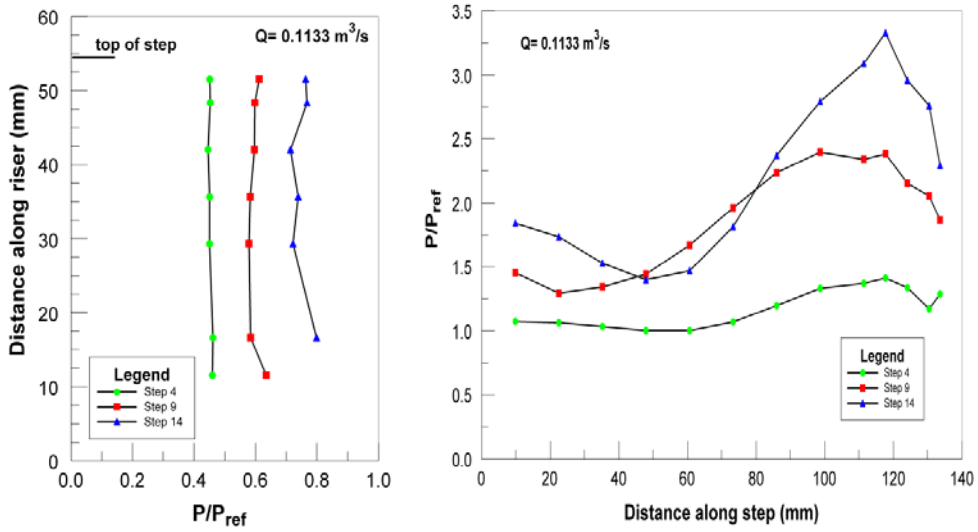

Figure 11: Pressures along step riser and tread for 50 mm steps at discharge 0.1133 m^3/s. Equivalent to the design discharge, 50.8 mm-high steps.

Similar data were collected with the 25 mm steps installed. Figure 12 shows the pressure gradient along the lid and figure 13 shows the pressures on a step for a discharge equivalent to the maximum for the spillway, 8835 m^3/s (312,000 ft^3/s).

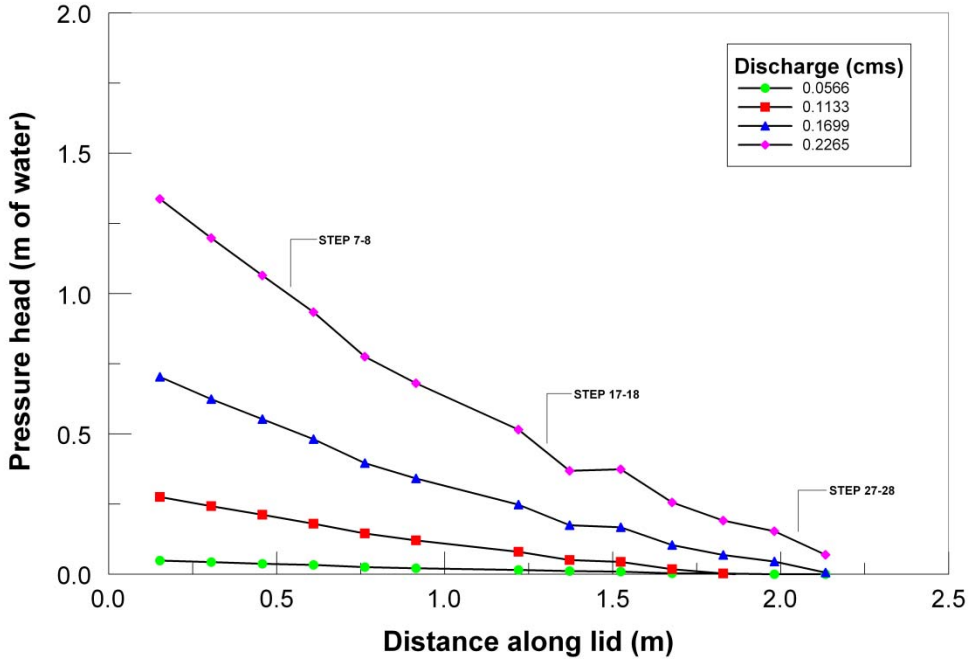

Figure 12: Pressure head on lid along stepped conduit (25-mm-high steps). Values of pressure at a specific discharge and step location are used as reference pressures.

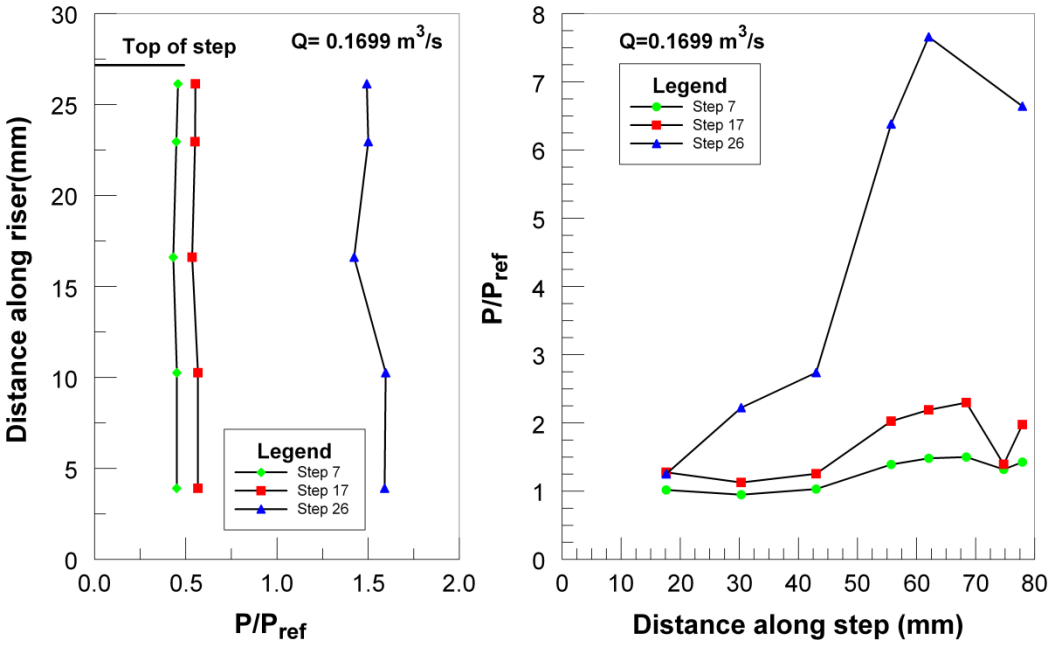

Figure 13: Pressures along step riser and tread25 mm steps - discharge 0.1699 m^3/s. Equivalent to the maximum discharge, 25.4 mm-high steps.

Sub-atmospheric Tests - LAPC

The stepped conduit was tested in a similar manner within the LAPC. Figure 14 presents the AE counts over 30 sec within a high frequency bandwidth (100 kHz- 1 MHz) as a function of cavitation index. The cavitation index was calculated using the local atmospheric pressure, the mean velocity in the conduit, and the reference pressure as discussed previously from the lid pressure gradient measurements on the lab floor.

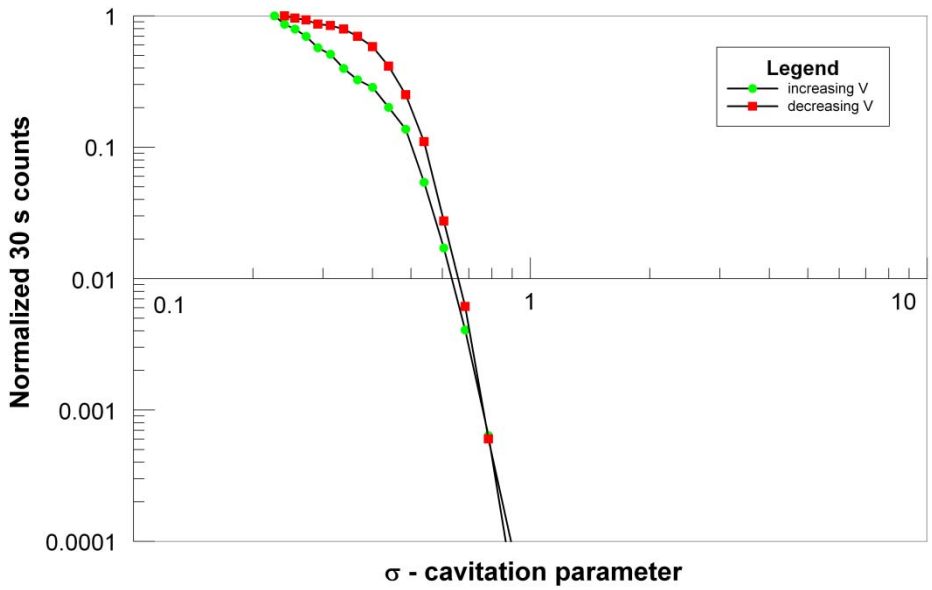

Figure 14: Normalized AE counts over 30 seconds in the HF bandwidth of 100 kHz-1 MHz for the 50.8mm-high steps.

The incipient value was chosen to reflect a normalized count of 1-percent for consistency in the determination method. This level, while not having a specific physical meaning, was the lowest value that resulted in acceptable repeatability in the incipient values. The AE sensor is extremely sensitive with several million counts during periods of heavy cavitation. The two curves show hysteretic characteristics in the data depending on whether the cavitation parameter was systematically decreased or increased. This hysteresis was not a big factor in determining the incipient value of 0.65, but seemed to have more influence at much lower sigma values. In addition to the AE data, high-speed video at a frame rate of 2000 Hz was collected. Video documentation focused on the end of the stepped conduit (step 13), incipient cavitation occurs first near the end of the conduit due to the aforementioned pressure gradient along the steps. Figures 15 a) and b) show the 50.8 mm steps at the incipient condition.

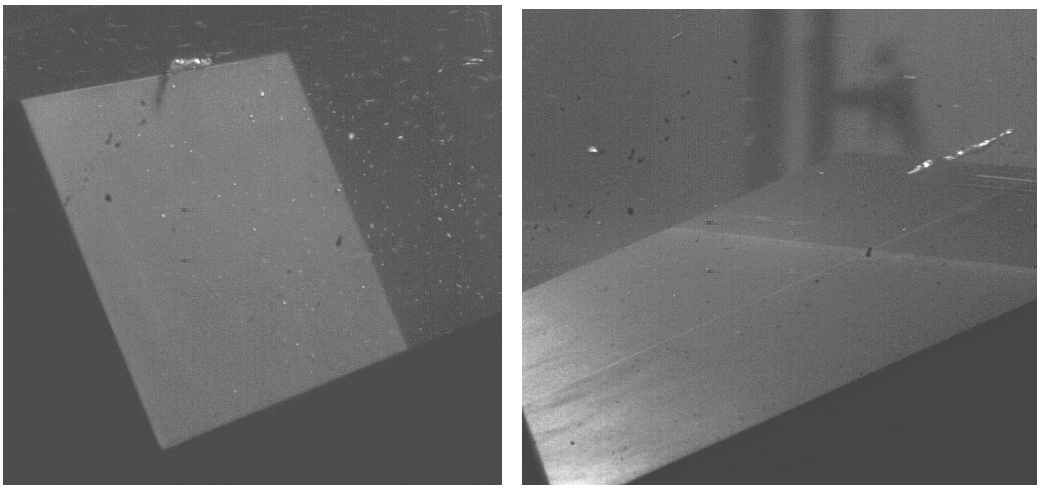

a) step riser **b) step tread**

Figure 15: Step riser and tread, flow from left to right showing incipient cavitation forming near the tip of the step and in the shear flow above the step tread. Vapor cavitiy appears in a streamwise tube or vortex oriented with the main flow. Flow sigma = 0.65 (50 mm step)

As the velocity was increased (cavitation parameter decreased) the level of cavitation and intensity increased. Figure 16 shows the large steps with a flow sigma of 0.46. Figure 17shows the increase of cavitation activity as the cavitation parameter is lower to 0.36.

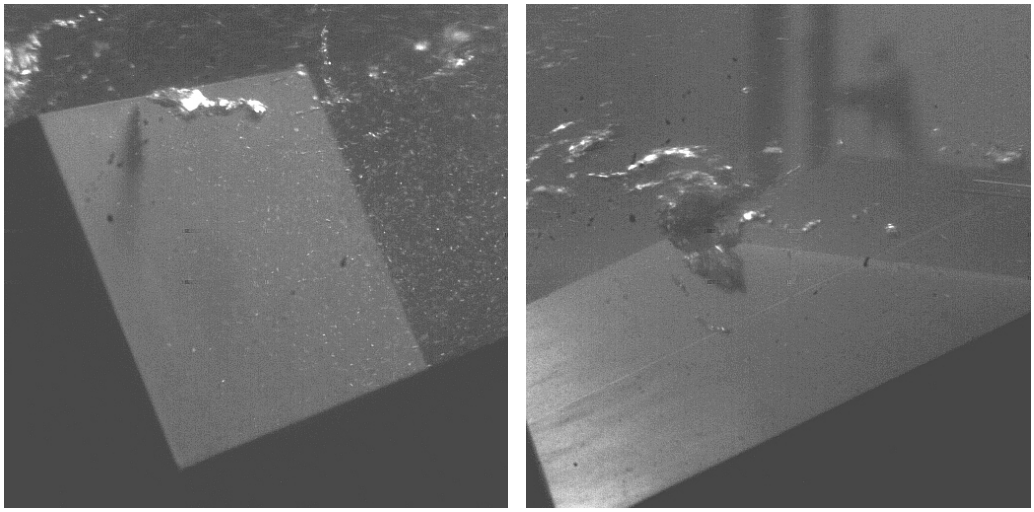

a) step riser **b) step tread**

Figure 16: Step riser and tread, flow from left to right showing cavitation at a flow sigma of 0.46. Note the flow within the recirculation zone on the step tread. (50 mm step)

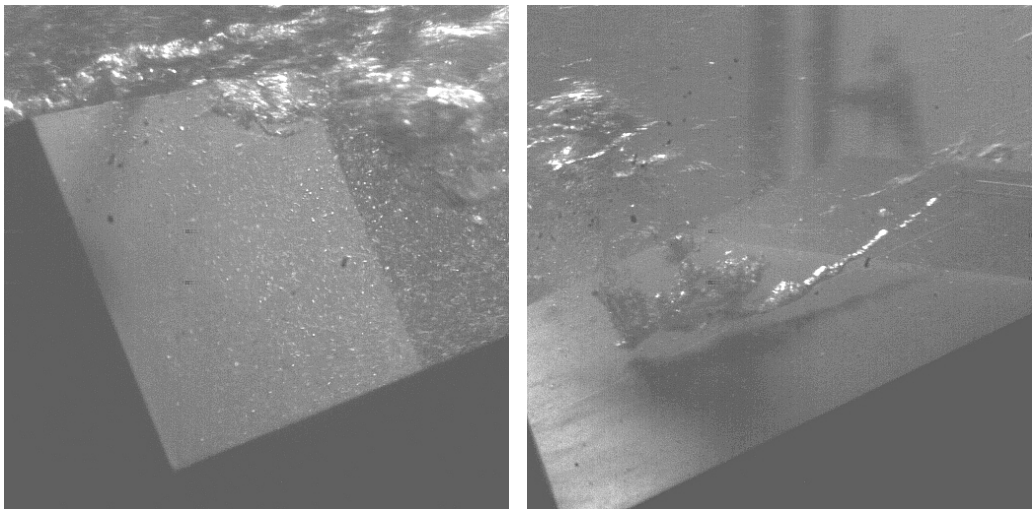

a) Step riser **b) Step tread**

Figure 17: The 50-mm-high steps at a flow sigma of 0.36. Note the increase in activity and the close proximity of the vapor bubbles and vortices to the surface of the step tread.

With the 25-mm-high steps installed into the conduit, the tests described previously were repeated. Figure 18 show the normalized AE counts as a function of the cavitation parameter.

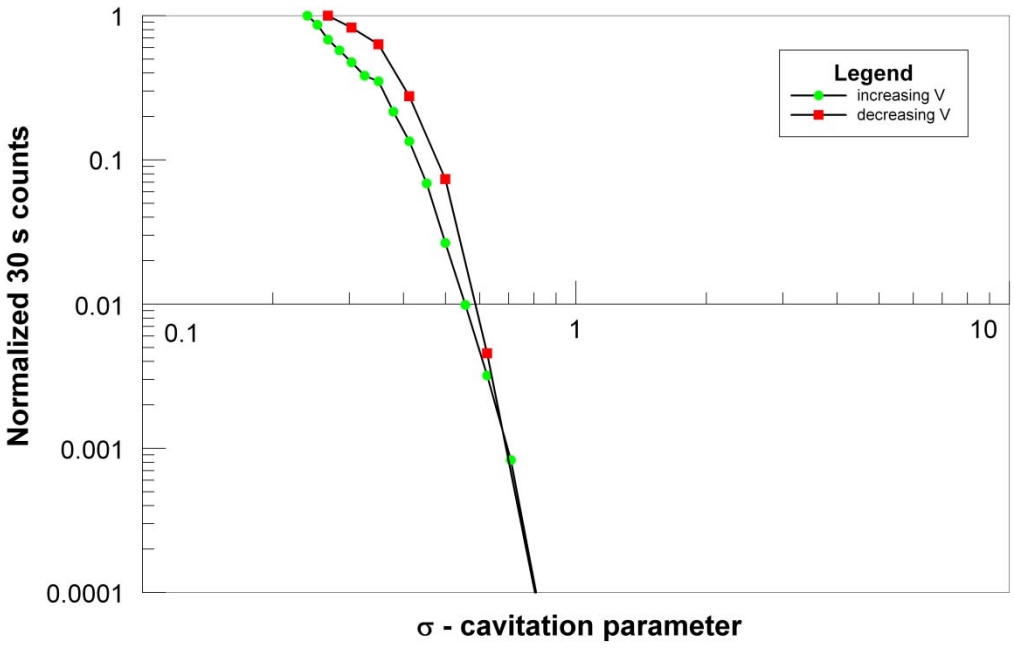

Figure 18: Normalized AE counts over 30 seconds in the HF bandwidth (100 kHz – 1 MHz) for the 25-mm-high steps.

Once again, from figure 18, we can pick off the value of the incipient cavitation parameter at a level of 0.01 normalized counts in 30 s. A mean value of 0.56 results for σ_i. Figure 19 shows the incipient condition in still photos captured from the high-speed video.

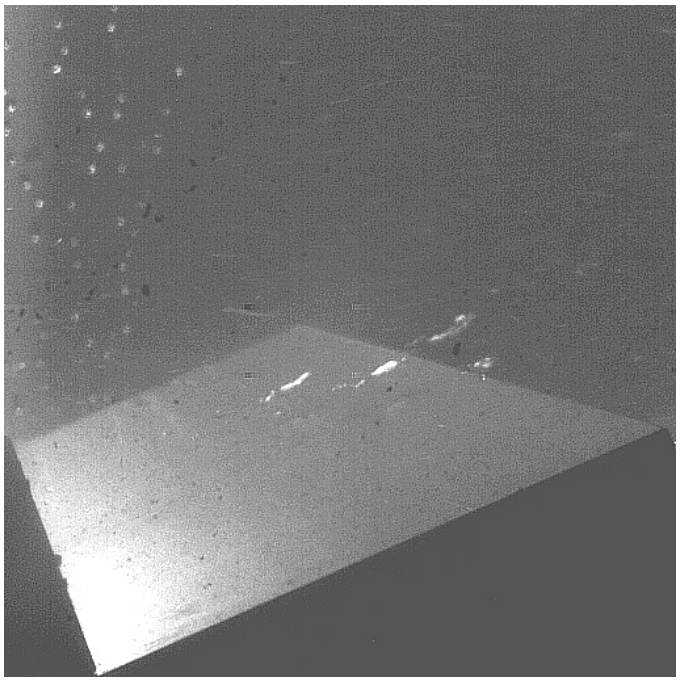

Figure 19: The 25-mm-high steps, flow from left to right showing incipient cavitation forming in the shear layer above the step. Vapor cavity is in the form of a tubular cavity or vortex oriented with the flow. Flow sigma = 0.52

As the velocity is increased, σ is lowered to 0.35, see figure 20. Figure 21 shows the steps from slightly above at an σ of 0.27, note combination of lateral and streamwise vortex/cavity formations.

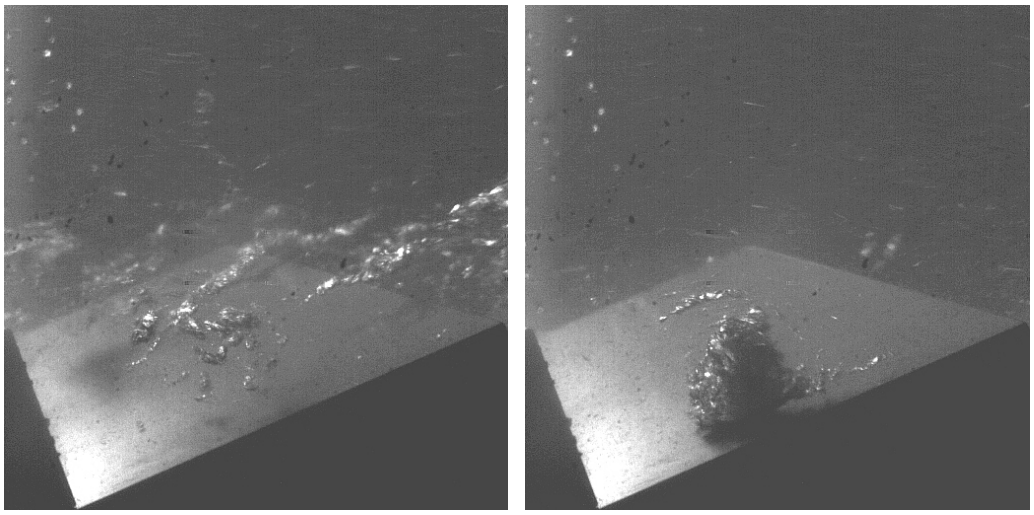

Figure 20: 25-mm-high steps at a flow sigma of 0.35. Left image shows streamwise oriented vortices while right image shows a large collection of vapor bubbles caught in the recirculation zone downstream from the step riser offset.

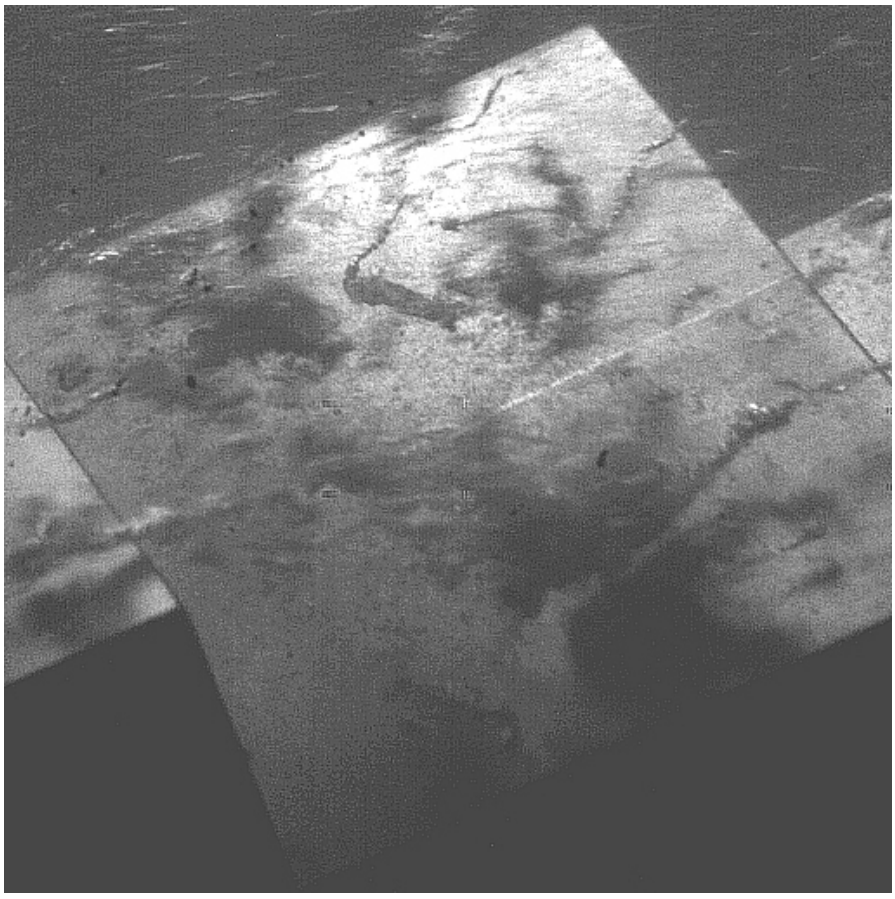

Figure 21: 25-mm-high steps at a flow sigma of 0.27. View is from slightly above. Flow is from left to right. Note streamwise vortex formation over the step tips with coalescence of vapor bubbles in the recirculation zone.

General characteristics of the cavitation formation and patterns are similar between the two step heights tested; however the incipient values were found to be significantly different with the larger steps having a higher incipient cavitation index.

Analysis and Discussion

Detailed hydraulic testing of stepped spillways has been accomplished by many researchers over the past 15-30 years. In general the emphasis has been on establishing the various regions of flow possible, the determination of energy dissipation characteristics of the steps, and the air entrainment resulting from typical open channel spillway flows. The JFP auxiliary spillway at Folsom Dam has many novel design features, including fully developed high-velocity flow entering the stepped section, relatively mild slope for such large discharges, and extremely high specific discharges (even at design flow). These issues contribute to uncertainties regarding the possibility for cavitation on the stepped spillway. While there are no existing installations that have reported cavitation damage on a stepped spillway, the design parameters for Folsom, in particular the resulting flow depths and specific discharges, are well beyond any designs currently in service. Sanchez-Juny et.al. [2008] used extensive dynamic pressure measurements from models to predict the possibility for cavitation inception on stepped chutes. Gomes et.al. [2007] used analysis of a developed pressure coefficient to predict

critical specific discharges in order to avoid cavitation inception. Pfister et.al. [2006] studied bottom aeration of stepped spillways as a means to prevent cavitation damage, although the presence of cavitation in the flow does not guarantee damage to the structure.

One approach to the design of stepped spillways has been to determine friction factors for various step configurations. Many researchers have taken this approach with quite a wide array of results and conclusions. Vittal, et.al.[1977] used an open channel and 2-dimensional triangular roughness elements (not unlike steps) to study the skin friction and form drag of undulating bed forms and dunes. Tozzi [1994] used a closed conduit with steps on the lower and upper surfaces and air as the fluid to measure and determine friction factors for a variety of step configurations. He then showed that these data could be applied to the more traditional open channel stepped spillway.

The perspective taken here involves two approaches: 1) using an overall or global approach measuring the pressure drop through the entire closed rectangular test section and determining a friction factor, weighting the factor to correct for only the bottom surface having roughness elements, and 2) Extracting velocity profile data from the PIV measurements along the steps and applying a logarithmic law of the wall approach to determine the friction factor. We did this for both the 50.8-mm and the 25.4-mm-high steps.

There are several different methods available to estimate friction factor, the most common being of the Darcy-Weisbach equation based on the total energy loss and a mean velocity. In order to adjust the friction factor to account for only one surface being covered with roughness elements, the methods followed by Boes and Hager [2003] can be applied. We further adjusted their weighting factor to account for a closed conduit, which involved an adjustment to the hydraulic radius. In addition, the Colebrook-White equation was also investigated, adjusting the relative roughness and the Reynolds number with a coefficient to account for the non-circular shape of the conduit. This coefficient was developed by Marchi [1961] who analyzed rectangular conduits with different aspect ratios.

Results of the different weighting methods for the friction factor and the two step heights are shown in Table 1.

Table 2: Comparisons of various methods to calculate global friction factor.

	50.8-mm-high steps	***25.4-mm-high steps***
Weighted Darcy-Weisbach	0.160	0.094
Boes & Hager f_b	0.130	0.073
Marchi/Colebrook-White	0.164	0.111

In addition, velocity profile information from the PIV measurements was also extracted in order to apply logarithmic fitting techniques commonly used. We have reported the logarithmic law integrated for circular conduits as the square cross-section of the test conduit is better represented by a circle than the “infinite” parallel plates used to develop the logarithmic law for rectangular sections. The application of these principles resulted in friction factors of 0.166 for the 50.8-mm steps and 0.091 for the 25.4-mm steps. This type of approach is termed a localized method as it uses specific velocity profiles from various locations along the conduit – again for the total range of discharges.

In an effort to apply the cavitation inception data collected in the LAPC to the Folsom auxiliary spillway, a 1-D single step method approach was used to calculate the cavitation parameter along the length of the spillway for the design and maximum flow conditions (Falvey [1999]). These data were provided to Reclamation by the COE – Sacramento District. Figure 22 shows the flow σ versus spillway stationing with the relevant incipient cavitation indices for the design flow and maximum flow condition. Our two roughness heights represent the relative roughnesses of the design flow and the maximum flow. It is noted that at the design flow, σ reaches the incipient cavitation number about 40 m upstream from the beginning of the constant sloped stepped section. With these conditions, it would be expected that cavitation likely would be present. Yet it is uncertain whether it would reach a damaging level. However for the maximum discharge, cavitation would be expected to form at the beginning of the steps and continue downstream. This includes the entire constant sloped section of the stepped chute (the geometry we studied). The photographic evidence of cavitation inception and development showed that the shear layer between the main flow skimming above the steps and the driven recirculating cavities were the most likely locations for cavitation to form. In addition the PIV measurements showing vorticity, rate of shear strain, and turbulent kinetic energy (figures 7 and 8) indicate the shear layer as the most probable location for cavitation. Figure 23 shows results from a computational fluid dynamics program that modeled the same test section where measurements were taken. This figure shows pressure contours overlain with flow streamlines, clearly showing the recirulation zone, the high pressure impact about ¾ down the length of the step tread, and finally the low pressure region just downstream from the step tips (along the vertical riser). The localized low pressures along with the dynamic flow features reinforce the likelihood that cavitation will form along this highly sheared region.

Cavitation formation within the stepped channel had many similarities to free shear layers studied by O'Hern [1987] and Baur and Köngeter [1998]. Both of their studies showed the formation of secondary streamwise vortices that were present during inception, somewhat characteristic of hairpin vortexes. These secondary vortices are due to instabilities that develop within the spanwise vortices that are part of the developing turbulent shear layer. The steps are not representative of a pure two-layer shear layer as these researchers studied and perhaps are a hybrid between a free shear layer and a wall-bounded shear layer. These streamwise cavitites (vortices) that appear first are stretched in the direction of flow but the relatively long length tends to support the notion that some type of vortical structure is present in order to maintain the thin tubular cavity.

The damage that may result from the formation of cavitation along the steps would be highly affected by air entrainment, as even small amounts of localized air concentration (7-percent) can effectively prevent damage [Peterka 1953]. Our experiments were carried out almost completely devoid of free gas within the water. This degassed condition is definitely not what the prototype structure would exhibit, but it allows for determination of the incipient cavitation index with repeatability in a laboratory setting. As flow on a stepped spillway has a multitude of nuclei for cavitation bubbles to form, we were not overly concerned with measuring nuclei concentrations in the laboratory. Consistent free surface air entrainment was not noted in the scaled hydraulic models that were used to study this structure. This isn't totally unexpected as air entrainment is known to have significant scale effects for scales greater than about 1:12 to 1:15 (it is Weber number dependant). The 1:26 model showed evidence of air entrainment in the form of turbulent bursts on the surface for the design flow but no air entrainment at the maximum discharge.

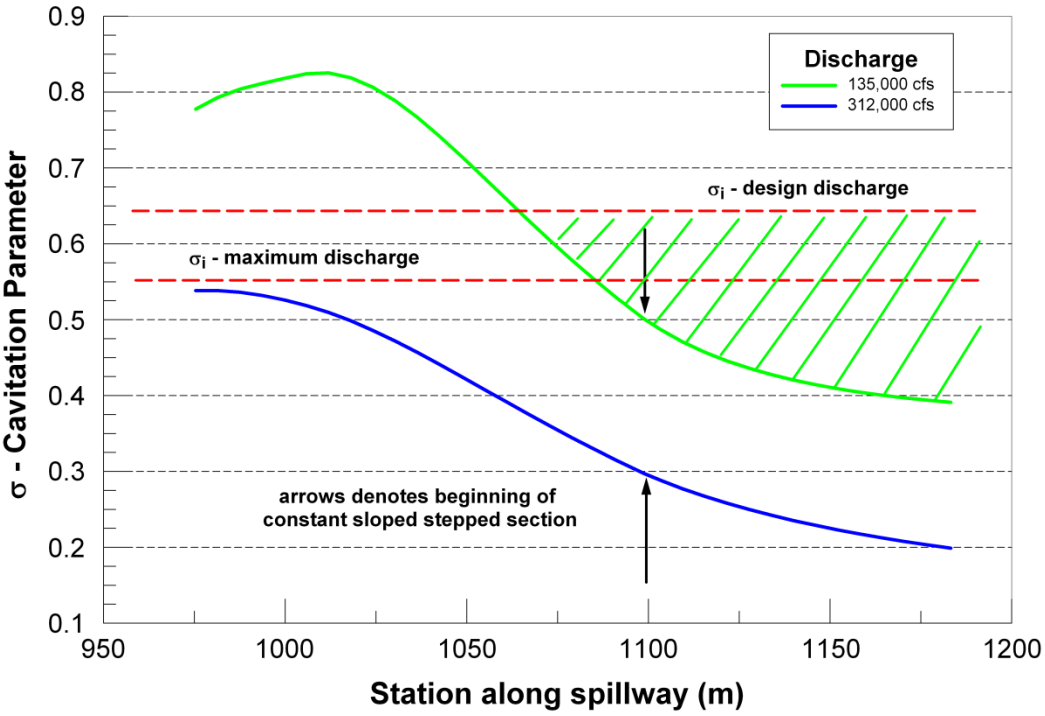

Figure 22: Flow σ versus spillway stationing for the design and maximum discharges. Incipient cavitation indices for each condition are noted. Entire stepped section is below incipient index for the maximum discharge

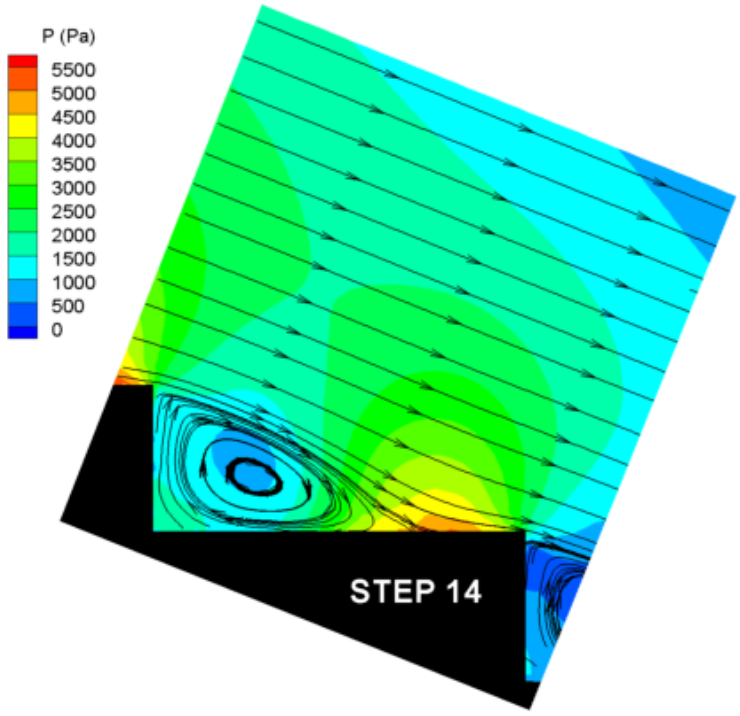

Figure 23: Computational fluid dynamics (Flow3D) results of a simulation for the experimental setup showing pressure contours and streamlines at step 14, 50.8 mm step.

Conclusions

Studies were conducted at the Reclamation hydraulic laboratory in Denver Colorado to measure the incipient cavitation index of the stepped spillway planned for the Joint Federal Project at Folsom Dam. This novel auxiliary spillway design has many features that have not normally been considered in stepped spillway designs previously so no prototype experience is available.

Friction factors were determined from tests at atmospheric conditions on the laboratory floor using pressure gradient measurements and velocity profiles extracted from Particle Image Velocimetry measurements. The two methods provided reasonable agreement and matched well with the design values that the USACE had used in their design calculations.

Cavitation studies were carried out in a specialized facility (LAPC) that allowed the lowering of the ambient pressure of the entire model to force cavitation formation at much lower flow velocities. The incipient cavitation index was found to vary with the friction factor.

At the design flow condition, which is the 200 year flood event, cavitation will likely occur along the constant sloped steps that were studied. Probable damage is difficult to predict as air entrainment is not easily predicted by present design guidelines. In addition, no actual damage was observed in the model – although the materials were very tough compared to the limited time of the runs. Predictions of damage from visual observations of the high-speed video images are still unproven. The maximum discharge should likely exhibit cavitation formation along the entire reach of the stepped portion of the chute and air entrainment is unlikely, increasing the probability for damage to occur.

References

Amador, A., Sanchez-Juny, M., and Josep Dolz, (2006). "Characterization of the Nonaerated Flow Region in a Stepped Spillway by PIV." *Journal of Fluids Engineering,* Vol. 128, pp. 1266-1273.

Baur, T. and J. Köngeter, (1998). "The three-dimensional character of cavitation structures in a turbulent shear layer." *XIX IAHR International Symposium on Hydraulic Machinery and Cavitation*, September, Singapore.

Boes, R.M. and W.H. Hager, (2003). "Hydraulic Design of Stepped Spillways." *Journal of Hydraulic Engineering,* Vol. 129, No. 9, pp. 671-679.

Chanson, H., (2001). "The Hydraulics of Stepped Chutes and Spillways." *Balkema Publications,* Rotterdam, The Netherlands.

Pfister, M., Hager, W.H., and H.E. Minor, (2006). "Bottom Aeration of Stepped Spillways." *J. Hydraulic Engineering,* Vol. 132, No. 8, pp. 850-853.

Falvey, H.T. (1990). "Cavitation in Chutes and Spillways." Engineering Monograph No. 42, Bureau of Reclamation, Denver, CO.

Gomes, J., Marques, M, and J.Matos, (2007). "Predicting Cavitation Inception on Steeply Sloping Stepped Spillways." *Proceeding of the XXXII IAHR Congress*, Venice, Italy, Tract C, Paper 1232.

Marchi, E., (1961). "Il moto uniforme delle correnti liquide nei condotti chiusi e aperti." *L'energia Electrica*, No. 5, pp. 393-413. (in Italian).

Matos, J. (2000). "Hydraulic Design of Stepped Spillways over RCC Dams." *International Workshop on Hydraulics of Stepped Spillways*, Zurich, Switzerland, H.E. Minor and W.H. Hager Editors, Balkema Publications, pp. 187-194.

O'Hern, T.J. (1987). "Cavitation Inception Scale Effects." Ph.D. Thesis, California Institute of Technology, Pasadena, California.

Ohtsu, I. and Yasuda, Y (1997). "Characteristics of Flow Conditions on Stepped Channels." *Proc. 27th IAHR Biennial Congress*, San Francisco, USA, pp. 583-588.

Peterka, A.J. (1953). "The Effect of Entrained Air on Cavitation Pitting." Proceedings of the Joint Meeting of the IAHR and ASCE, Minneapolis, MN.

Sanchex-Juny, M., Blade, E., and J. Dolz, (2008). "Analysis of pressure on a stepped spillway." *Journal of Hydraulic Research*, Vol. 46, No. 3, pp. 410-414.

Tozzi, M.J., (1994). "Residual energy in stepped spillways." *International Water Power & Dam Construction*, May 1994, pp. 32-34.

Vittal, N., Ranga Raju, K.G., and R.J. Garde, (1977). "Resistance of Two Dimensional Triangular Roughness." *Journal of Hydraulic Research*, Vol. 15, No. 1, pp. 13-36.